

Chapter 8

Continuous Wet Granulation



Arwa El Hagrasy, Li Ge Wang, and Jim Litster

Abstract Wet granulation is a critical unit operation in solid dosage form manufacturing in the pharmaceutical industry. Traditionally, wet granulation has been a batch process. Recently, there has been a move toward more advanced manufacturing approaches such as continuous processing to allow more rigorous process control, consistent quality assurance, and reduced capital costs. This chapter discusses continuous wet granulation process with emphasis on twin screw granulation as the most commonly used continuous granulation approach in the pharmaceutical industry. The key design features of a twin screw granulator (TSG) are described, and comparisons with batch high shear granulation equipment are made. The effects of formulation and process variables on granule attributes are discussed. Mechanistic studies of screw elements with the proposed granulation rate processes are presented. Real-time process monitoring tools, including spectroscopic and imaging techniques, are described. Implementation of dimensional analysis as a tool for scaling up/scaling out of continuous twin screw granulation is presented. Two numerical methods, that is, population balance model (PBM) and discrete element method (DEM), are chosen for the multiscale modeling of twin screw granulation, and their coupling mechanisms of data exchange between DEM and PBM are discussed.

Keywords Continuous wet granulation · Process design and process control · Twin screw granulation · Population balance model · Discrete element method · Granulation rate processes · Residence time distribution

The opinions and conclusions expressed in this chapter are solely the views of the authors and do not necessarily reflect those of the Food and Drug Administration.

A. El Hagrasy
Office of Pharmaceutical Manufacturing Assessment, Office of Pharmaceutical Quality,
CDER, FDA, Silver Spring, MD, USA

L. G. Wang · J. Litster (✉)
Chemical and Biological Engineering, University of Sheffield, Sheffield, UK
e-mail: James.Litster@sheffield.ac.uk

Nomenclature

a	Particle radius, mm
b_M	Breakage function
$B(v, t)$	Birth rate, $m^{-3} s^{-1}$
B_{agg}	Birth rate of agglomeration, $m^{-3} s^{-1}$
B_{break}	Birth rate of breakage, $m^{-3} s^{-1}$
B_{nuc}	Birth rate of nucleation, $m^{-3} s^{-1}$
C_{impact}	Impact frequency, s^{-1}
d_p	Particle diameter, mm
D	Barrel diameter, mm
$D(v, t)$	Death rate, $m^{-3} s^{-1}$
D_{break}	Death rate of breakage, $m^{-3} s^{-1}$
$D_{m_p, nuc}$	Death rate of powder particles, $kg m^{-3} s^{-1}$
d_{50}	Median size of feed particle, mm
F_n	Series of geometric ratios
F_{powder}^{in}	Flow rate of additional powder stream, $kg s^{-1}$
G	Growth rate, s^{-1}
G_m	Maximum growth rate, s^{-1}
G_{shear}	Shear rate, s^{-1}
h	Interparticle gap, mm
k	Compaction rate constant, s^{-1}
l	Liquid volume, m^3
L	Barrel length, mm
$\dot{L}_{in, powder}(x, t)$	Rate of liquid addition to the fine powder, $kg h^{-1}$
m	Mass of particle, kg
M_{powder}	Mass of fine powder, kg
$M_{granule}$	Mass of granule, kg
\dot{m}_p	Mass flow rate of powder, kg/h
\dot{m}_l	Mass flow rate of liquid, kg/h
n	Population density of length function, m^{-3}
P_1	Rate coefficient
P_2	Size-dependent exponent
St_v	Stokes deformation number
$V_{droplet}$	Volume of a single liquid droplet, m^3
V_{nuc}	Volume of particle in saturated granule, m^3
$V_{L, nuc}$	Volume of liquid in saturated granule, m^3
V_p	Per-particle pore volume, m^3
S_1	Volume of solid component 1, m^3
S_2	Volume of solid component 2, m^3
$S_M(w, v)$	Specific breakage rate, s^{-1}
x_w	Moisture content of powder
x_{wc}	Critical moisture content of powder
Δx	Reduction of particle size

σ	Standard deviation
ω	Angular velocity of the shaft, rads^{-1}
ε	Granule porosity
ε_{bed}	Powder bed porosity
ε_{min}	Minimum granule porosity
ρ_b	Particle density, kg m^{-3}
u_0	Collision velocity, ms^{-1}
μ	Binder viscosity
LSR	Liquid/solid ratio
PFN	Powder feed number
Fr	Froude number

8.1 Introduction

In contrast to some other unit operations such as roll compaction and tableting, wet granulation in the pharmaceutical industry has traditionally been a truly batch process, undertaken in mixing equipment borrowed from the food processing industry. By far the most common batch granulator designs are vertical shaft high shear mixers, with a smaller number of horizontal shaft mixers also used (Hapgood et al. 2007).

In other industry sectors, continuous wet granulation is standard and most often used in high-throughput applications in mineral processing, fertilizers and industrial chemicals, and detergents. Tumbling granulators (drums and pans), fluidized bed granulators, and horizontal axis high shear mixers have all been used in continuous mode (Litster and Ennis 2004). The main driver in these industries for continuous processes is economies of scale. Therefore, standard equipment designs for these industries have throughputs from 1 to 100 tonne hr^{-1} and are much too large for pharmaceutical applications. In moving from batch to continuous processing, the pharmaceutical industry had to look for continuous processing options with much lower capacities in the range 5–50 kg hr^{-1} . Once again, the industry borrowed equipment from another application – twin screw extruders used for polymer extrusion.

Figure 8.1 gives an illustration of a twin screw granulator (TSG). Powder and liquid are added separately to the twin screw barrel. Multiple addition points are possible. The wet granulation mass is conveying forward down the barrel. In contrast to operation as an extruder, there is no die plate, and the powder state is more akin to that in a screw feeder. In most of the barrel, the powder fill is low and there is no buildup of pressure along the barrel. Granules flow freely out of the end of the barrel and usually drop directly into a fluid bed drier. There is great flexibility in the choice of the length and configuration of the corotating screws with a wide variety of screw elements available for use including standard conveying elements (CE), kneading elements (KE), and distributive mixing elements (DME).

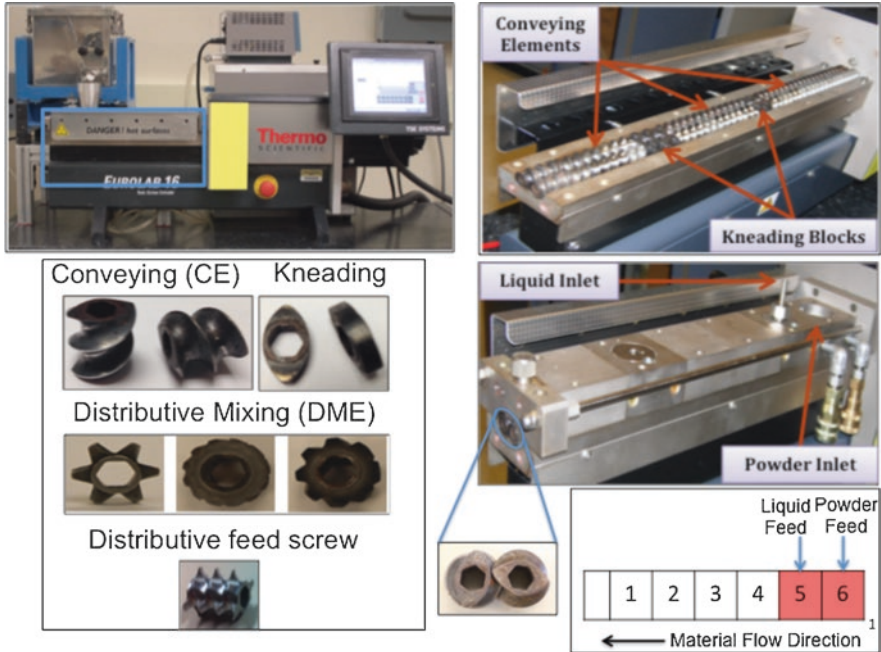


Fig. 8.1 Illustration of the key features of a twin screw granulator

The TSG has a number of intriguing features that contrast markedly from batch high shear wet granulation. The residence time in the granulator is short (5–20 s), and the pressure applied to the granules is low so that granules are high porosity, relatively weak, and not spherical. The confined nature of the barrel means good liquid distribution via a spray nozzle is not possible. Liquid is typically added via a jet or drips from a simple orifice so that bimodal granule distributions are common. Alternative methods of binder addition have been reported including foam granulation (Tan and Hapgood 2012) and melt binder (Mu and Thompson 2012). However, addition of liquid through a simple orifice is by far the most common in practice. The granules in the barrel are conveyed forward with limited back mixing. When combined with the ability to customize screw elements along the barrel, this gives the opportunity to develop a regime-separated granulator (Mu and Thompson 2012). The balance of rate processes in a TSG is very different to that in a HSWG, and TSG performance is much less sensitive to changes in formulation properties. Table 8.1 highlights the characteristics of continuous twin screw and batch high shear granulators and the very different products they produce.

In the following sections, we describe the controlling rate processes for granulation in a TSG, the impact of formulation, and process parameters on performance. The state of the art for process modeling of TSG is described and scale-up issues are discussed.

Table 8.1 Contrasting characteristics of twin screw granulation and high shear mixer granulation

HSWG characteristics	TSG characteristics
Batch process	Continuous process
Can handle a wide variety of powder and liquid feeds	Can handle a variety of powder and liquid feeds, but capacity may be limited by powder flow properties
Batch size up to 200 kg for 300 l granulator	Throughput up to 25 kg hr. ⁻¹ for 25 mm barrel size
Batch times of 2–20 minutes	Residence time 5–20 seconds
Produces medium to high density granules	Produces low to medium density granules
Performance is sensitive to formulation properties	Performance is not sensitive to formulation properties
Coupled densification and growth are key rate processes	Breakage and layering are key rate processes
Changes to equipment are difficult	Screw configuration is easy to change leading to regime-separated granulation designs
Scale up through 3 or 4 scales from development to manufacturing. Granule properties difficult to maintain during scale-up	Development and manufacturing can be done at the same scale by increasing the continuous campaign time while keeping granule properties constant

8.2 Process Design and Characterization

8.2.1 Formulation and Process Variables

Effect of Binder Delivery Method/Binder Content and Delivery Method

The granulating binder in a twin screw granulation (TSG) process can be delivered in the powder phase, liquid phase, or a mixture of the two. The preferred method of binder delivery in TSG will depend on formulation properties as well as screw configuration. Formulation properties will define the rate of wetting, penetration, and spreading of the binder. Screw configuration determines the extent of shear imparted on the granulated material inside the TSG, which provides the energy needed to spread the granulating liquid and form liquid bridges between the particles.

El Hagrasy et al. observed that the use of solubilized binder reduced the level of fines and resulted in a narrower granule size distribution (GSD) compared to the dry binder delivery when using conveying elements (CE) and kneading elements (KE) in the screw configuration (El Hagrasy et al. 2013a). The short residence time in the TSG may prevent complete solubilization of the dry binder, thereby reducing its binding capacity compared to the dry form. Recent reports examined the impact of binder distribution and granulating liquid viscosity on granule properties and process attributes (Saleh et al. 2015; Dhenge et al. 2012a). The presence of binder in the liquid phase increases the viscosity of the granulating liquid, therefore increasing the liquid penetration time in a static bed. In the absence of adequate shear forces inside the granulator as in the case of CE, the less viscous granulating

liquid, that is, binder in the dry phase, produces narrower GSD due to faster spread and penetration of the droplets. The addition of KE increases the shear during granulation, resulting in a relatively more even distribution of the viscous binder solution and less difference in granule properties between the different binder delivery methods.

Dhenge et al. also examined the effect of incorporating increasing concentrations of binder in the liquid phase on granule attributes (Dhenge et al. 2012a). Higher binder concentrations in the liquid phase increase the viscosity of the granulating liquid. As a result, stronger liquid bridges bind the particles forming a larger median size of the granules. X-ray tomography images of the internal structure revealed less voids at higher binder concentrations. The residence time distribution (RTD) also increased when using higher liquid binder concentration, further contributing to the densification of the formed granules.

Considering that the mean residence time inside TSG is in the order of seconds, careful consideration of both the binder delivery method and the screw configuration used is important to ensure adequate distribution of the binder during granulation and desired granule attributes for downstream processing.

Effect of L/S Ratio

The variation in L/S ratio during granulation impacts the GSD obtained during TSG. El Hagrasy et al. reported that increasing L/S ratio initially shows a gradual increase in the ratio of coarse granules to ungranulated fines while maintaining the bimodal distribution characteristic of the TSG process (El Hagrasy et al. 2013a). Figure 8.2 shows a typical frequency distribution as a function of L/S ratio. The screw configuration was a combination of CE and KE. The broad granule size distribution obtained with TSG has been reported by other researchers as well, using a similar screw configuration (Dhenge et al. 2010; Djuric and Kleinebudde 2008, 2010; Djuric et al. 2009; Keleb et al. 2004; Van Melkebeke et al. 2008).

Per the nucleation regime map reported by Hapgood et al. for other types of granulation equipment, the operating regimes are defined by two dimensionless groups, namely, the dimensionless spray flux and the dimensionless drop penetration time (Hapgood et al. 2003, 2007). Due to the confined space inside a TSG, the granulating liquid is dripped directly into the powder inside the barrel. The relatively large droplets obtained compared to a spraying addition mode place the TSG nucleation process in the mechanical dispersion regime, which relies on shear forces for adequately distributing the granulating liquid. The broad bimodal size distribution of the granules at moderate L/S ratios points to inefficient liquid distribution by the standard screw elements typically used in TSG such as CE and KE.

Further increase in L/S ratio transfers the process into a rapid growth regime, where a rapid increase in d_{50} and a narrower monomodal GSD are observed. Nevertheless, the granule attributes, in terms of size, shape, and porosity, obtained at such high levels of L/S ratio will likely obviate their use in downstream pro-

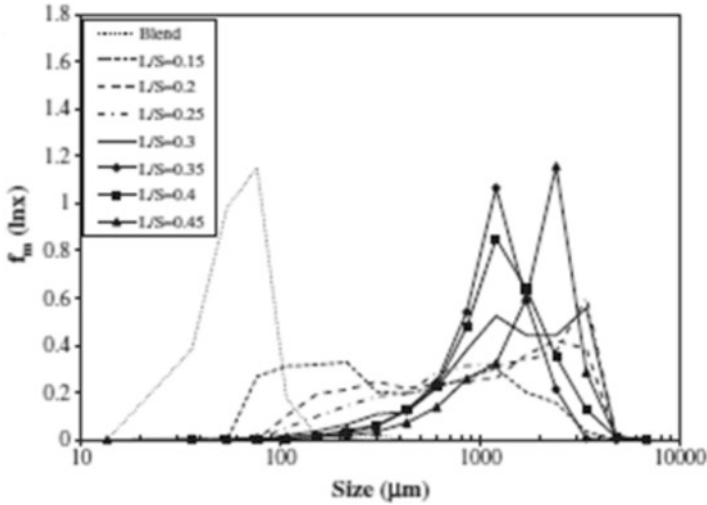


Fig. 8.2 The change in size distribution of granules obtained from a TSG process at different L/S ratios. (Adapted from El Hagrasy et al. (2013a))

cesses. The higher liquid content increases the deformability of the granules, yielding large elongated granules with dense structures.

Effect of Operating Channel Fill Level

The channel fill level inside a TSG depends on the material feed rate, screw speed, and the specific geometry of the screws and barrel. For a given screw configuration, variation in material feed rate and screw speed have opposite effects on the material holdup inside the granulator and thus the degree of channel fill (Kumar et al. 2014; Seem et al. 2015). Higher material input rate into TSG lowers the degree of channel fill, whereas higher screw speed decreases the degree of channel fill. The screw configuration affects the degree of channel fill because of the difference in the free volume available in the barrel, depending on the screw geometry used. CE generally offer more free volume than other types of mixing elements, thereby allowing for less restrictive flow of material through the granulator. With mixing elements, such as KE or distributive mixing elements (DME), the free volume will depend on the number of elements as well as the offset angle used. Thus, the fill level will also vary in the axial direction of the granulator, depending on the screw configuration along the shaft (Lee et al. 2012).

Recent studies characterizing the mixing dynamics inside the TSG using positron emission particle tracking (PEPT) and near-infrared (NIR) chemical imaging techniques allowed a faster sampling rate and thus more in-depth understanding of material transport inside the granulator and how it is impacted by operating parameters such as screw speed, material input rate, and screw configuration (Kumar

et al. 2014; Lee et al. 2012). Within the material flow rate and screw speed suitable for PEPT (10–20 g/min and 150–300 rpm, respectively), Lee et al. concluded that the RTD decreases with the increase in screw speed and material feed rate. The increase in offset angle was generally shown to increase the RT because of more restricted flow. However, normalized RTD curves and Peclet numbers revealed no difference in the degree of axial mixing at the studied variables of screw speed, material feed rate, and screw configuration. Kumar et al. quantified their RTD results in terms of the mean RT (t_m), the Peclet number (Pe), and the normalized variance (σ^2_θ) as a descriptor of the extent of axial mixing. The impact of screw speed and material input rate on RT observed using NIR chemical imaging by Kumar et al. was consistent with the PEPT study, where higher screw speed and material input rate reduced the (t_m). However, the analysis of (σ^2_θ) and Pe showed that varying material feed rate, screw speed, number of mixing elements, and their offset angles resulted in substantial variation in the mixing behavior. Plug flow was enhanced by low screw speed, high material feed rate, number of KE, and their offset angle. Although a higher number of KE and/or offset angle increase RTD, the material flow was hindered due to the restrictive flow imparted by the large number of KE combined with the low screw speed. Kumar et al. further studied the mixing dynamics inside the TSG and its impact on solid-liquid mixing and GSD as a function of screw speed, material throughput, L/S ratio, number, and offset angle of KE (Kumar et al. 2016). The study demonstrated that despite high axial mixing observed in certain experiments, yet the granule attributes were not optimal due to increase in the level of fines and coarse granules, an indication of insufficient liquid distribution characteristic of KE (El Hagrasy et al. 2013a; El Hagrasy and Litster 2013).

While the specific results in the literature were not always consistent, the overall conclusion is that the parameters impacting the degree of channel fill have a substantial effect on mixing behavior, material flow, and the resulting granule attributes. It is thus important to optimize the granulation operating parameters in an integrated CM process to allow sufficient degree of dispersive mixing and adequate liquid distribution in the granulator to achieve desired granule attributes. Mechanistic understanding of granulation rate processes, RTD characterization, and imaging techniques becomes important tools in this regard because they allow in-depth understanding of the impact of those parameters. Characterization of granulation process dynamics through RTD studies is particularly valuable in defining the optimum process and equipment design parameters that avoid plug flow and allow sufficient operational time to yield adequate liquid distribution.

8.2.2 Mechanistic Studies and Screw Characterization

Screw configuration has a strong impact on granule attributes in a TSG process. There are different screw designs available for use with a TSG. The early literature in this area has mostly described the use of CE and KE combinations, which are

originally adopted from the extrusion literature (Thiele 2003). The use of mixing elements has also been described in the TSG literature (Sayin et al. 2015a). The modular design of a TSG allows innumerable number of possible screw configurations, making screw configuration one of the most complex equipment design parameters in a TSG.

The output granule properties from a TSG are the result of granule evolution along the length of the TSG. Therefore, mechanistic understanding of granule formation, using different screw element designs and their combinations, is essential to optimizing the TSG process. Characterizing the impact of individual screw elements on different granule attributes provides a framework for the development of multidimensional PBM that can be implemented for future process optimization and control.

Conveying Elements (CE)

CE are helical-shaped screw elements known for their excellent transport properties and so are typically positioned at the inlet of liquid/solid material into the TSG and to transport material to or from different mixing zones. The powder in CE is subjected to minimal shear compared to other mixing zones in the granulator, which plays an important role in defining granule properties in this section as described later. CE design variables that determine channel volume and extent of drag flow include:

1. Flight pitch: axial distance between the tip of two adjacent flights.
2. Flight lead: axial displacement corresponding to one turn of the flight.

The effect of design variables of CE on granule properties was studied by different research groups (Djuric and Kleinebudde 2008; Thompson and Sun 2010). In general, larger element pitch provided smoother and more even feeding to subsequent elements at a given flow rate. However, GSD was essentially similar (within experimental error) across the length of the CE, indicating minimal influence of CE on granule attributes.

Granulating liquid is dripped into the conveying section during operation, leading to granule formation by immersion since the liquid drop is substantially larger than the powder primary particles (Dhenge et al. 2012b). El Hagrasy and Litster demonstrated that a bimodal size distribution of ungranulated fines and wet agglomerates is generally produced (El Hagrasy and Litster 2013). The wet agglomerates represent the nuclei formed during the initial wetting step, and the higher L/S ratio leads to droplet coalescence and formation of a higher fraction of the large agglomerates. Figure 8.3 shows that the fraction of coarse granules to fines varied depending on the L/S ratio, with a higher fraction of coarse granules obtained at higher L/S ratios. However, minimal liquid distribution and shape transformation occurred in this section regardless of the L/S ratio used.

Granule growth in CE was also found to be dependent on viscosity of the granulating liquid (Dhenge et al. 2013). The lower viscosity of the granulating liquid

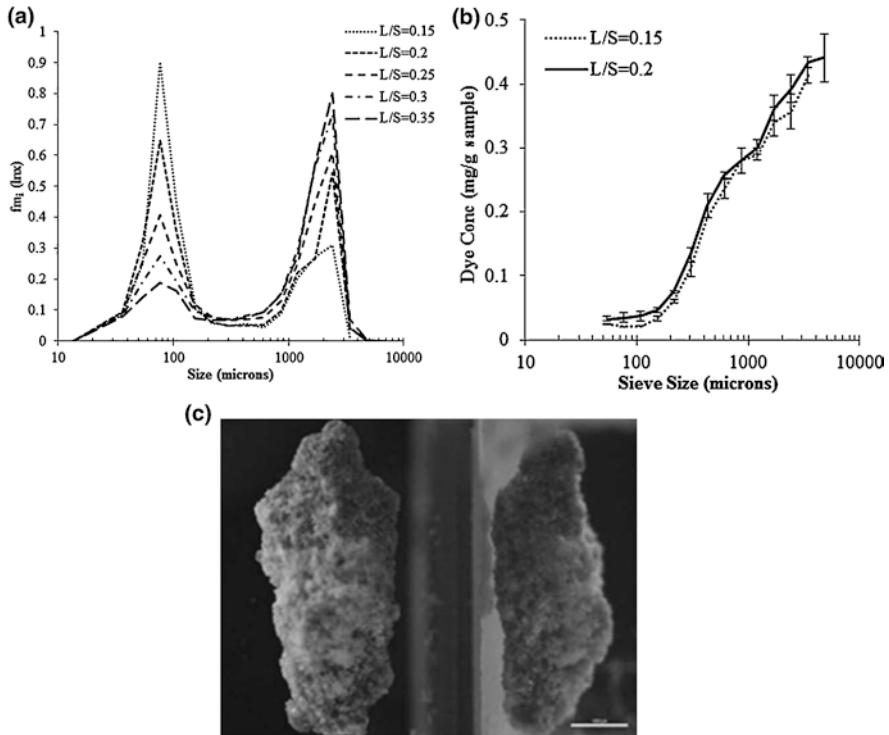


Fig. 8.3 (a) The change in size distribution of granules from the conveying section at different L/S ratios, (b) dye concentration in the different size fractions of granules from the conveying section; the error bar at each data point is the standard deviation of three measurements; (c) micrographs of top (left) and side (right) view of a representative granule from the conveying section. (Adapted from El Hagrasy and Litster (2013))

resulted in shorter liquid penetration time and relatively better granulating liquid distribution, leading to fewer small granules (<710 microns) and a larger fraction of medium and coarse granules (710–1000 microns and >1000 microns). Dhenge et al. linked the granulation process in the CE section of a TSG to flow behavior of dry and wet material with varying degrees of channel fill. Particle image velocimetry (PIV) and DEM studies showed that dry powder demonstrated the highest average particle velocity. The velocity decreased with the addition of low viscosity binder solutions, for example, water, because of increased cohesiveness of the formulation and subsequent dissipation of kinetic energy from the screws. Alternatively, the velocity behavior of the formulation approached that of dry powder as the viscosity of the granulating liquid increased due to the poor wettability ameliorated by the low shear environment in this zone.

The impact of material throughput in the CE section on granule size was less definitive and could not be generalized across different studies, where some reported an increase in the level of fines, while others reported the opposite effect (Djuric and

Kleinebudde 2008, 2010; Thompson and Sun 2010; Dhege et al. 2013; Liu et al. 2015) The inconsistency among different studies could be attributed to the sensitivity of granule formation in this zone due to the low shear environment encountered, resulting in more pronounced impact of formulation, process, and equipment design parameters. Nevertheless, the design of CE upstream of the granulating elements, for example, KE, did not play a role in the granule attributes obtained downstream of KE (Liu et al. 2015). However, the CE used downstream of the kneading section influenced the granule properties with the studied 60F KE configuration.

Mixing Elements (KE and DME)

In a typical TSG operation, CE are used in combination with other types of mixing elements that provide the adequate shear and liquid distribution to produce granules suitable for downstream processing. Kneading elements (KE) provide a dispersive mixing zone for the incoming material from the conveying section, resulting in densification and breakage of large agglomerates and varying degrees of liquid distribution.

KE design variables: The KE configuration can be characterized in terms of (El Hagrasy and Litster 2013; Thompson and Sun 2010; Li et al. 2014):

1. Number of KE: defines the length of the kneading section.
2. Advance angle: offset angle between each successive pair of KE. Most common angles are 30, 45, 60, or 90. The AA defines the gap volume, which is the space in the middle channel between the tips of each pair of KE per the isometric drawings in Fig. 8.4. The divergence in the middle channel is expressed in terms of the diameter (D) of the barrel.
3. Angle orientation: forward (F) or reverse (R) depending on the rotational direction of the KE tips with respect to the flight of the preceding CE. The diagrams in Fig. 8.5a, b display the front view of the forward and reverse angle directions of KE at 60°, respectively.

El Hagrasy and Litster provided a detailed report on the impact of design variables of KE, including offset angle, angle orientation, and length of kneading section on granule physical properties and liquid distribution (El Hagrasy and Litster 2013). Figure 8.6 summarizes the dominant mechanisms occurring in the CE and KE sections of the TSG that govern the size, shape, and liquid distribution of the resulting granules. The two main granulation rate processes occurring in the kneading section can be summarized by:

1. Breakage, followed by layering.
2. Shear-elongation and breakage, followed by layering.

Breakage was the dominant mechanism in the 90° configuration, whereas shear-elongation was dominant in the 30 °R configuration. Other configurations demonstrated different degrees of combination between the two mechanisms. The breakage mechanism in 90° configuration can be attributed to the frequent intersection of the

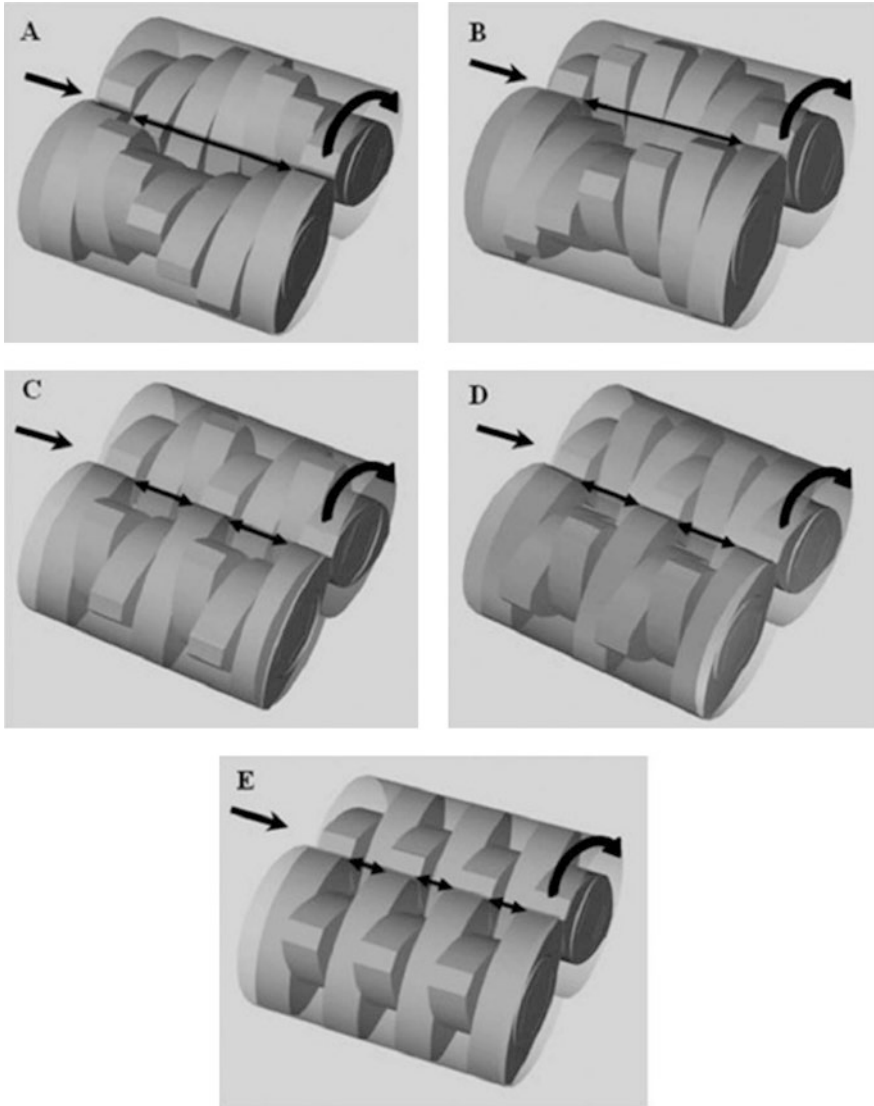
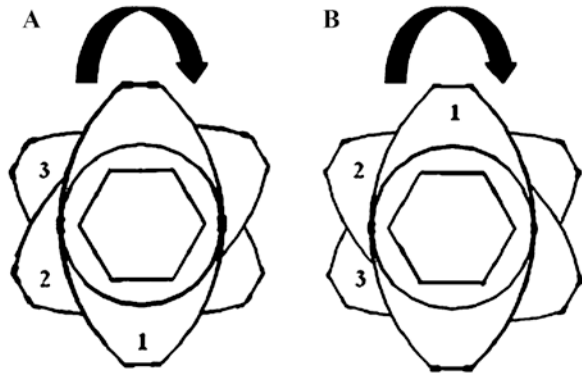


Fig. 8.4 Configurations of kneading section using 7 KE at (a) 30 °F, (b) 30 °R, (c) 60 °F, (d) 60 °R, and (e) 90°. The curved arrow indicates the direction of rotation of the shafts, and the straight arrow depicts the direction of material flow from the CE into the kneading section. The middle channel divergence length illustrated by the double-headed arrow is 1.25D for (a) and (b), 0.5D for (c) and (d), and 0.25D for (e). (Adapted from El Hagrasy and Litster (2013))

KE tips in the middle channel more than any other KE configuration (Fig. 8.6e). Breakage creates new wet surfaces that can pick up dry fines, thereby improving LD. The use of more KE in the 90 configuration enhances the breakage events, leading to simultaneous creation of more fines and improvement of LD.

Fig. 8.5 Two-dimensional (2D) front view of the screw configuration for 3KE60 in the (a) forward angle direction and (b) reverse angle direction. The incremental order of KE shows the elements from front to back. The curved arrow indicates the directions of rotation of the shafts. (Adapted from El Hagrasy and Litster (2013))



Screw Type	Dominant Rate Processes	More KE	
		Liquid Distribution	Granule Growth
	Drop Nucleation (DN)	NA	NA
Conveying	Layering High L/S Ratio Droplet Coalescence Layering	NA	NA
Neutral	Breakage Layering	+	-
Reverse	30° Shear-Elongation and Breakage	+	+
	60° Layering Shear-Elongation and Breakage + Layering Breakage + Layering	+	+
Forward	30° Breakage + Layering + Conveying characteristics	+	+
	60° Conveying characteristics	Nil	Nil

NA: Not applicable + Positive Change - Negative Change Nil: No Change

Fig. 8.6 Proposed granulation rate processes in a twin screw granulator. (Adapted from El Hagrasy and Litster (2013))

In the reverse configurations, such as 30R and 60R, the wet agglomerates from the CE are smeared against the barrel wall. The shear-elongation mechanism, characteristic of 30 °R and 60 °R, improves liquid distribution inside TSG, especially with the addition of more KE. However, the resulting granules are dense with an undesirable flake-like shape that will likely cause powder handling problems during downstream processing. Other configurations demonstrated bimodal granule size distribution because of poor liquid distribution and/or breakage events, which requires the use of a downstream milling step of oversized granules to ensure drying homogeneity and avoid powder segregation issues.

Distributive mixing elements (DME), also known as comb mixing elements, are another type of mixing elements used in the TSG that have been studied by many researchers (Djuric and Kleinebudde 2008, 2010; Thiele 2003; Sayin et al. 2015a; Thompson and Sun 2010). Mixing in DME is attained through a series of cutting and recombination of inflowing granular material. Sayin et al. characterized the granulation rate processes in this type of mixing elements (Sayin et al. 2015a). The researchers investigated the impact of both screw orientation (forward versus reverse) and placement (adjacent versus spaced) on the resulting granule attributes. Figure 8.7 illustrates the design of the DME described in this work.

Liquid distribution and granule size significantly improved with the DME in the reverse orientation, regardless of placement. However, granule shape and porosity were not affected by DME orientation or placement. Flow visualization and RTD studies using a high-speed imaging camera showed that the reverse orientation improved the breakage of incoming granular material, leading to better liquid distribution through exchange between broken lumps and ungranulated fines. The dominant granulation rate processes occurring in the DME section are illustrated in Fig. 8.8.

Fig. 8.7 Front view (a) and side view (b) of a distributive mixing element. (Adapted from Sayin et al. (2015a))

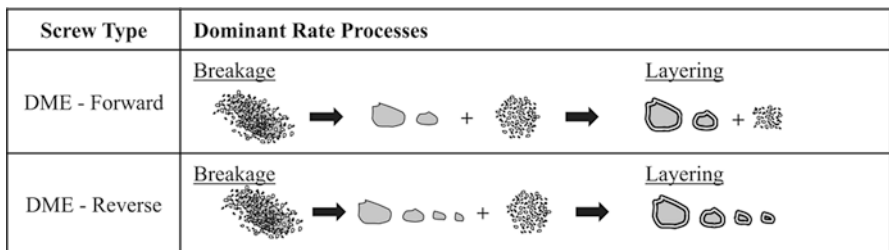
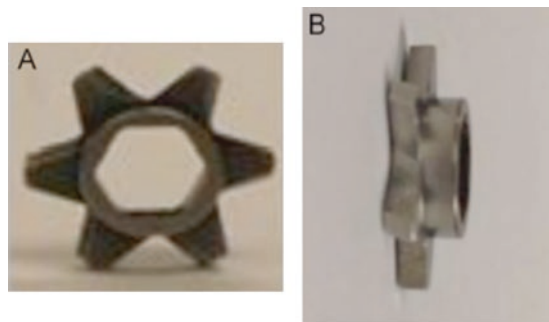


Fig. 8.8 Proposed granulation rate processes in distributive mixing elements in a twin screw granulator. (Adapted from Sayin et al. (2015a))

In contrast to KE, DME offer the potential of producing granules with more desirable attributes for downstream processing, including:

1. Monomodal size distribution without lumps that obviates the need for a downstream milling step.
2. Spherical-shaped porous granules with potentially improved flow properties.

The collective knowledge from the different studies used in characterization of screw elements in a TSG and the modeling work for simulation of the impact of screw configuration on granule attributes are yet to be utilized in optimizing the design of screw elements and configuration in a TSG process. To take it one step further would be to understand how to manipulate the functional role of different screw elements to custom-design desired granule attributes for different pharmaceutical applications a priori.

8.3 Real-Time Process Measurement and Process Control

In addition to the use of adequate science and engineering principles in process design, real-time process monitoring, implementation of process models, and process control tools are indispensable for continuous manufacturing. Real-time process measurement tools enhance process understanding that allows improved process design and optimization. The continuous monitoring of the process also ensures acceptable product quality throughout the manufacturing process. The real-time measurement of critical quality attribute (CQA) allows necessary process adjustments with minimal disruption of the continuous manufacturing line or diversion of nonconforming product without running the risk of rejecting the entire run.

NIR and Raman spectroscopy were used to examine the possibility of real-time measurement of solid-state changes of the active ingredient during twin screw granulation (Fonteyne et al. 2013). The spectroscopic measurements were collected on a static sample of granules at the outlet of the granulator. In addition, an in-line probe was placed in the stream of wet granules for particle size analysis. Both spectroscopic techniques provided an understanding of the impact of process parameters on the solid state of the active ingredient, with Raman technique showing more sensitivity than NIR in this study. However, probe fouling posed a challenge in using the particle size analyzer for in-line measurement of particle size distribution.

In-line monitoring of changes in granule size during a twin screw granulation process as a function of variation in process and formulation parameters was examined in another study (El Hagrasy et al. 2013a, b). An imaging camera (Eyecon™) was used to collect 3D surface maps of the sampled particles. An iterative process was then used to determine the equivalent diameter of the projected particles, from which the volume distribution was derived. The authors implemented statistical process control tools to evaluate the utility of different camera outputs,

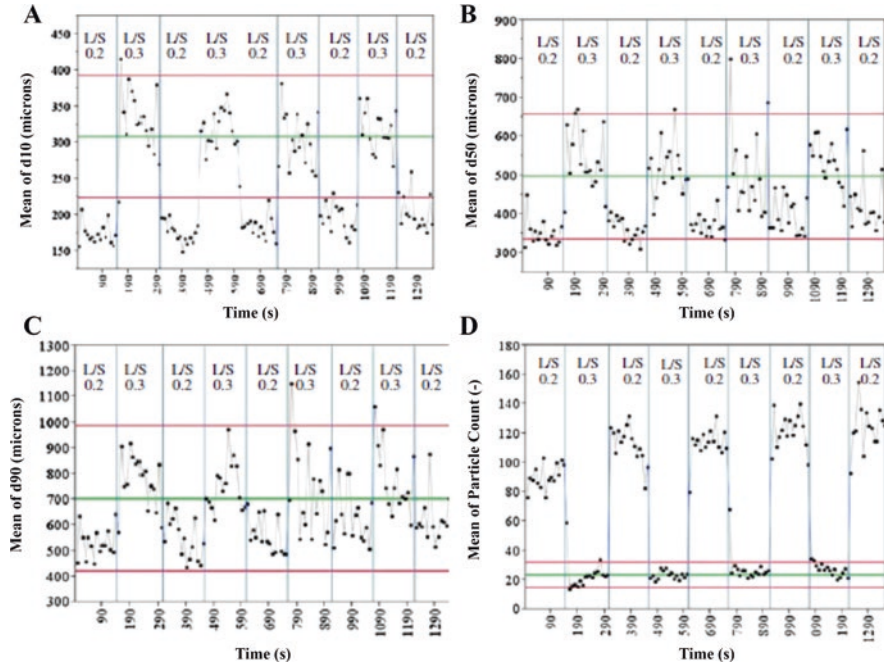


Fig. 8.9 Shewhart control limits applied to (\bar{X}) charts of d_{10} (a), d_{50} (b), d_{90} (c), and particle count (d). The upper and lower horizontal lines depict the upper control limit and lower control limit, respectively. The centerline depicts the process mean. The vertical lines mark the onset of change in L/S ratio. (Adapted from El Hagrasy et al. (2013b))

including statistics of particle diameter (d_{10} , d_{50} , and d_{90}) and particle count for granulation process monitoring and control. Figure 8.9 illustrates the (\bar{X}) charts for d_{10} , d_{50} , d_{90} , and particle count, in which the respective parameter in each case is plotted as a time series.

Particle count and d_{10} demonstrated the most robust performance among all studied particle quality characteristics. Unlike other calculated parameters such as d_{50} and d_{90} , d_{10} and particle count had inherently low measurement variability. Thus, they were more sensitive to changes in granule size attributes during routine process monitoring. An additional study from the same group confirmed the utility of this online technique with TSG (Sayin et al. 2015b).

Future optimization of the GSD characteristics from a TSG process is expected to further enhance the data quality obtained from direct measurement of granules using the camera or other process analyzers. Alternatively, such process monitoring tools can be interfaced with a downstream milling process to monitor milled granule size.

Moisture content is an important quality attribute of granules produced by a wet granulation process, especially that some formulations require tight control of moisture content to ensure optimal tablet characteristics. In-line NIR spectroscopy

was used for moisture content measurement on an integrated continuous granulation-fluid bed drying-milling process (Chablani et al. 2011). The NIR spectra were collected from a granule transfer hopper module situated between the fluid bed dryer and the mill. The work demonstrated the feasibility of using NIRS for measuring moisture content real time during processing.

However, the dynamic range of the calibration developed was limited because of the study design, in which the spectra were collected after the completion of the drying process. In another study, Fonteyne et al. placed the probe in the second cell of a six-cell segmented fluid bed dryer (Fonteyne et al. 2014). The probe placement earlier in the drying process allowed the variation in process parameters to produce sufficient difference in moisture levels. The calibration model developed was more robust due to wider range of moisture content values, and model validation showed that the NIR method was equivalent to the reference analytical method. Thus, it is important to carefully consider sensor-equipment interface with the continuous process to ensure that representative samples are collected for calibration development, validation, and method implementation.

Besides measuring granule attributes and physicochemical properties, process analytical technology (PAT) tools were also utilized to understand TSG process dynamics and material transport through measurement of RTD (Kumar et al. 2014, 2016; Vercruyse et al. 2014). Digital video recording was also used for measuring RTD in TSG (Sayin et al. 2015a; Li et al. 2014). Real-time process measurement tools provide an advantage over manual sampling techniques for measuring RTD, considering the relatively short residence time inside a TSG (Thompson 2015). Characterization of RTD is important for optimization of equipment design, formulation, and process parameters to achieve the desired degree of axial mixing (Gao et al. 2012). Experimental RTD measurement starts by adding a tracer to the inlet of the granulator when operating at steady state. The real-time sensor is then used to measure the signal from the tracer as it emerges from the granulator. The measured RTD represents the degree of axial dispersion along the length of the granulator covered in the study. Direct measurement of RTD is also possible through particle tracking using PEPT (Lee et al. 2012). In addition to measuring RTD of the entire screw length, it also provides RTD measurements within individual screw elements if desired.

8.4 Scaling Up and Scaling Out

Scaling up of continuous twin screw granulation is less of a concern than for batch HSWG because development work and manufacturing can often be done on machines of identical size and design. Smaller or larger amounts of product are simply made by running the equipment for shorter or longer periods of time. As the residence time in the TSG is of order 5–20 s, only a few minutes is needed to reach steady state. When undertaking a DOE for development work, the TSG need only be held a one set of conditions for 10–15 minutes to collect data, and quite short run

times are needed to provide product for clinical trials. For manufacturing, the campaign time can be many hours or even several days if required. This time-based “scaling out” is common.

Nevertheless, scale-up is sometimes necessary. The smallest available TSG systems have a barrel diameter of 11.2 mm, and equipment with barrel diameters of 16 mm, 24 mm, 25 mm, and 50 mm are available from different manufacturers. In addition, during scale-out, operators may wish to increase productivity by increasing the powder feed rate when compared to development operations, sometimes with corresponding increase in screw speed. So the important question remains: How do granule properties (critical quality attributes) vary with:

1. Changes to powder feed rate and screw speed for a given screw geometry and powder.
2. Changes to powder properties for given screw geometry and operating conditions.
3. Changes in screw barrel diameter for geometrically similar twin screws?

When considering scale-up and scale-out, dimensional analysis is a powerful tool. If we consider process parameters only, such an analysis leads to the following relationship between key dimensionless groups (Osorio et al. 2016):

$$\frac{d_{50}}{D} = g_1 \left(LSR, PFN, Fr, \frac{L}{D}, F_1, F_2, \dots \right) \quad (8.1)$$

$$\varepsilon = g_2 \left(LSR, PFN, Fr, \frac{L}{D}, F_1, F_2, \dots \right) \quad (8.2)$$

where ε is granule porosity and LSR is the liquid to solid ratio:

$$LSR = \frac{\dot{m}_l}{\dot{m}_p} \quad (8.3)$$

PFN is the powder feed number:

$$PFN = \frac{\dot{m}_p}{\rho_b \omega D^3} \quad (8.4)$$

and Fr is the Froude number:

$$Fr = \frac{D\omega^2}{2g} \quad (8.5)$$

Here D is the barrel diameter, ω is the angular velocity of the shaft, L is the barrel length after wetting addition of liquid, \dot{m}_p and \dot{m}_l are the mass flow rates of the powder and liquid, respectively, ρ_b is the bulk density of the powder, and F_1, F_2, \dots

are a series of geometric ratios that describe the geometry of the individual screw elements and the screw configuration.

If scale-up will be undertaken by keeping important geometric ratios similar (e.g., L/D for the whole TSG and for each screw element used), Eqs. (8.1) and (8.2) can be simplified to:

$$d_{50} = D \cdot g_1(LSR, PFN, Fr) \quad (8.6)$$

$$\varepsilon = g_2(LSR, PFN, Fr) \quad (8.7)$$

PFN is the ratio of the volumetric powder feed rate to the turn over of volume in the screw barrel as the screw turns. It is closely related to the fill level in the barrel. Given the confined nature of the TSG and the screw operation, as screw speed or powder feed rate changes, the powder residence time changes very little with the fractional fill level adjusting up and down to match the change in PFN . Fr is an important parameter in mixer granulators, where it dictates the powder circulating pattern and mixing. However, it is less important for the TSG where operation is typically well below the critical value for centripetal flow.

Osorio et al. (2016) showed that the key granule attributes (d_{10} , d_{50} , d_{90} , ε) were largely insensitive to PFN and Fr . This is good news for scaling out in the same equipment. Granule attributes are highly sensitive to LSR , and care should be taken to keep LSR constant when scaling out. As predicted by Eqs. (8.1) and (8.6), the granule size distribution parameters, especially d_{90} , increase with increasing barrel diameter (see Fig. 8.10). This is because the largest granule size is that which can survive breakage events. For the TSG, breakage events are defined by the screw element geometry, and the largest gap through which a granule can pass unbroken will scale with barrel diameter for geometrically similar screw elements. Thus when scaling up, it will not be possible to keep the same granule size distribution, with the size of larger lumps increasing directly with scale.

In contrast, granule porosity is scale invariant and generally higher than achieved in HSWG. For a given formulation, porosity is sensitive only to LSR .

In summary, performance of the TSG during scaling out is robust with respect to both process parameters and formulation properties, except for LSR . We expect this will continue until a critical value of PFN when the free volume in the most constraining screw element section becomes completely full with powder and the TSG blocks. Anecdotally, we have observed that the critical PFN can be a function of both the screw element configuration and the powder flow properties. However, there are no rigorous published studies to confirm this. For free flowing powders, stable performance is possible over a wide range of screw speeds and powder flow rates.

Scaling up to larger screw barrels presents challenges in controlling the largest granule size. However, granule porosity does not change with barrel diameter and is robust on scale-up.

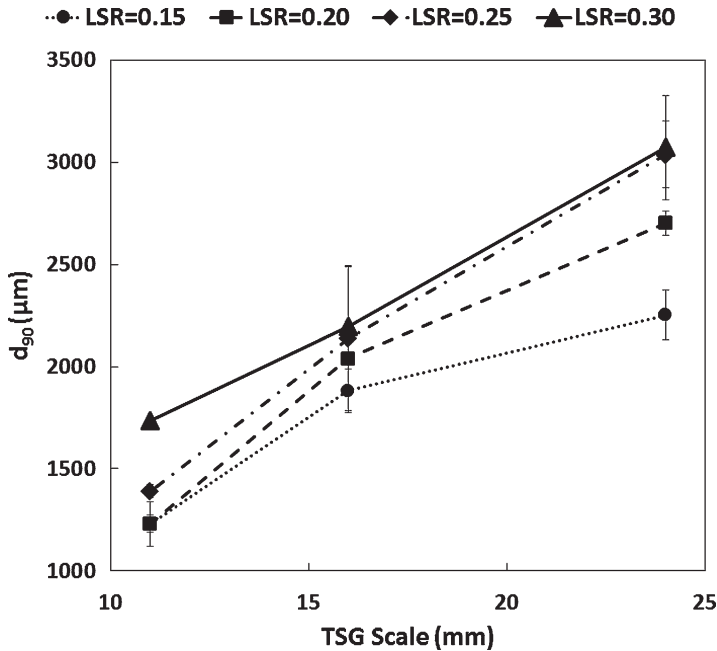


Fig. 8.10 Effect of TSG scale (barrel diameter) and LSR on d_{90} [$PFN = 1.30 \times 10^{-2}$] (Osorio et al. 2016)

8.5 Population Balance Model (PBM) of Twin Screw Granulation

8.5.1 A Generic Expression of the Population Balance Model

The population balance model (PBM) is a series of integrodifferential equations which describe the dynamic evolution of particles with respect to a certain attribute. The population balance model has been extensively used to model the granulating process as the particles are subjected to rate processes such as consolidation, aggregation, and breakage. For a well-mixed batch system with only one attribute (particle volume) considered, the population balance model is given by (Randolph and Larson 1971; Hounslow et al. 1988):

$$\frac{\partial n(v,t)}{\partial t} + \frac{\partial}{\partial v} [Gn(v,t)] = B(v,t) - D(v,t) \quad (8.8)$$

where $n(v, t)$ is the number density function, v is the vector representing particle property (herein volume), G is the growth rate, and $B(v, t)$ and $D(v, t)$ are the functions to denote the birth and death of particles due to aggregation, breakage, and nucleation.

Most PBMs in the literature are one-dimensional, which typically considers one particle property with regard to size (Barrasso et al. 2014). 1D PBM is limited in accuracy for predicting the real process of granulation due to the lack of variation of liquid binder and porosity. Consequently, multidimensional PBMs have been developed to incorporate the three properties: solid, liquid, and gas volume. A 3D population balance model evolves based on Eq. (8.8) (Poon et al. 2008):

$$\begin{aligned} \frac{\partial}{\partial t} n(s, l, g, t) + \frac{\partial}{\partial s} \left[n(s, l, g, t) \frac{ds}{dt} \right] + \frac{\partial}{\partial l} \left[n(s, l, g, t) \frac{dl}{dt} \right] + \frac{\partial}{\partial g} \left[n(s, l, g, t) \frac{dg}{dt} \right] \\ = B_{\text{nuc}}(s, l, g, t) + B_{\text{agg}}(s, l, g, t) + B_{\text{break}}(s, l, g, t) - D_{\text{break}}(s, l, g, t) \end{aligned} \quad (8.9)$$

where (s, l, g) is the vector representing the solid, liquid, and gas volume of a granule and $n(s, l, g, t)$ is the population density of a granule with the three vectors over time. The three terms, with regard to partial differential functions, refer to the state change due to solid layering, liquid addition, and gas consolidation, respectively. $B_{\text{nuc}}(s, l, g, t)$ and $B_{\text{agg}}(s, l, g, t)$ denote the net rates of nucleation and aggregation. $B_{\text{break}}(s, l, g, t)$ and $D_{\text{break}}(s, l, g, t)$ denote the birth and death rate due to breakage, respectively.

Multicomponent formulations are standard in the pharmaceutical industry, and 3D PBM falls short of accounting for granule composition. Alternatively, one or more granule properties could be lumped into the remaining distributions in a reduced-order model (Hounslow et al. 2001). Another approach is proposed to add the fourth dimension (multicomponent) into the 3D population balance model. A 4D PBM was developed by Barrasso (2015) in the light of 3D PBM in Eq. (8.10). It gives:

$$\begin{aligned} \frac{\partial}{\partial t} n(s_1, s_2, l, g, t) + \frac{\partial}{\partial l} \left[n(s_1, s_2, l, g, t) \frac{dl}{dt} \right] + \frac{\partial}{\partial g} \left[n(s_1, s_2, l, g, t) \frac{dg}{dt} \right] \\ = B_{\text{agg}}(s_1, s_2, l, g, t) + B_{\text{break}}(s_1, s_2, l, g, t) - D_{\text{break}}(s_1, s_2, l, g, t) \end{aligned} \quad (8.10)$$

where s_1 and s_2 are the volumes of two solid components in the granule. $B_{\text{agg}}(s_1, s_2, l, g, t)$, $B_{\text{break}}(s_1, s_2, l, g, t)$, and $D_{\text{break}}(s_1, s_2, l, g, t)$ are the net rates of aggregation, birth, and death rate due to breakage, respectively. Note that the nucleation and layering effects are excluded from this model.

8.5.2 Rate Process Kernels in Twin Screw Granulation

Design of the twin screw granulation differs from the traditional granulators where all the rate process kernels take place in a single granulation container. In the twin screw granulation however, due to its regime-separated nature, different rate process

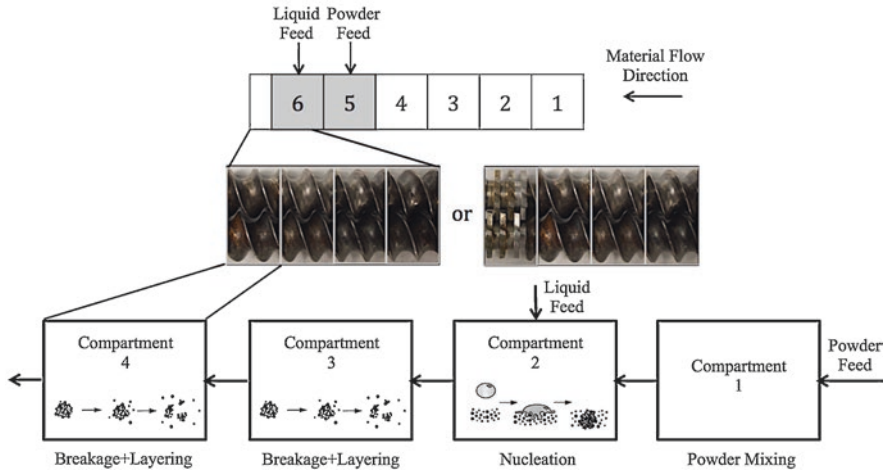


Fig. 8.11 Compartment-based rate mechanisms in a twin screw granulation (Sayin 2016)

kernels should be defined for each compartment. In Fig. 8.11, an example of the compartmental population balance modeling approach is depicted where rate mechanisms are specified based on the screw configuration.

The first compartment is the powder mixing zone in which no rate process kernel is defined. The second compartment is the conveying element where the liquid drips down to form nuclei with nucleation kernel considered. The third compartment is still the conveying element where the mixture of liquid and powder is transported. The fourth compartment is composed of either conveying element or a combination of other elements (KE or DME). In both the third and fourth compartment, the breakage and layering kernels are considered, whereas the agglomeration kernel is ignored due to the short residence time in the compartment. Considering the rate process kernels required in the population balance modeling of twin screw granulation, the key equations of nucleation, breakage, consolidation, and layering are presented below.

Nucleation Kernels

The nucleation mechanism takes place in the compartment where the droplet is fed into the powder bed. The rate of nuclei formation, B_{nuc} , is equal to the rate of droplet addition to the powder fines (Barrasso and Ramachandran 2016):

$$B_{nuc} = \frac{\dot{L}_{in,powder}(x,t)}{V_{droplet}} \tag{8.11}$$

where $L_{in,powder}(x, t)$ is the rate of liquid addition to the fine powder and $V_{droplet}$ is the volume of a single liquid droplet, which is assumed to be constant and spherical.

It is assumed that each droplet reaching fine particles forms a single saturated granule with volume V_{nuc} and liquid volume $V_{L, \text{nuc}}$. During nucleation, solid material grows to form a granule due to the transfer from the fine powder phase. The death rate of fine powder particles, $D_{m_p, \text{nuc}}$, is equal to the product of the nucleation rate and the mass of solid associated with each nucleus (Barrasso and Ramachandran 2016):

$$D_{m_p, \text{nuc}} = \frac{\dot{L}_{\text{in, powder}}(x, t)}{V_{\text{droplet}}} (1 - \epsilon_{\text{bed}}) V_{\text{nuc}} \rho_s \quad (8.12)$$

where ϵ_{bed} is the powder bed porosity and ρ_s is the density of the solid.

Breakage Kernels

The mass-based breakage equation is primarily used in the form (Hill and Ng 1995):

$$\frac{dM(v, t)}{dt} = \int_v^\infty S_M(w) b_M(v, w) dw - S_M(v) M(v, t) \quad (8.13)$$

where $M(v, t)$ is the mass of particles with volume v at the time t , $S_M(w)$ and $S_M(v)$ are the specific breakage rates of mass fraction of particles of volume w and v , and breakage function $b_M(v, w)$ denotes the fragment size distribution probability between the volume range v and w . $b_M(v, w) = B_{v-1, w} - B_{v-1, v}$.

The breakage kernel is composed of two important functions, namely, the selection function (S_m) and the breakage function (B_m). The selection function represents the breakage rate of particles, while the breakage function represents the breakage size distribution after collision. The selection function has been mainly studied in the application of milling. It should be noted that the majority of these selection functions are empirical and applicable to brittle material milling tests. However, their applicability to the breakage probability of granules in the wet granulation has not yet been fully tested. In terms of selection function used in the twin screw granulation, Barrasso et al. (2015a) proposed a size-dependent kernel including two fitting parameters P_1 and P_2 :

$$S_M = \frac{1}{2} G_{\text{shear}} P_1^{P_2} \quad (8.14)$$

where G_{shear} is the shear rate, P_1 is a rate coefficient, and P_2 is a size-dependent exponent.

The breakage function used in the twin screw granulation is given by Barrasso and Ramachandran (2016):

$$b_M(v, w, v', w') = 2\delta\left(v - \frac{v'}{2}, w - \frac{w'}{2}\right) \quad (8.15)$$

This fragment size distribution assumes that particles undergoing breakage would be broken into two equally sized particles. In another study by Sayin (2016), using the two equal volume fragments produces fairly good agreement in the conveying elements. However, a big deviation of the granule size prediction was found with the distributive mixing elements.

A recent study of breakage-isolated experiment in the twin screw granulation by Pradhan et al. (2017) indicates that the dominant breakage mechanisms in conveying and distributive mixing elements are chipping and fragmentation, respectively. This necessitates the development of different breakage kernels based on the screw elements. Furthermore, the critical granule size pertinent to the screw geometry beyond which the breakage probability increases dramatically was identified. The critical breakage size was determined as the largest available gap size by measuring the screw elements' open volume geometry.

Consolidation Kernels

Ennis et al. (1991) considered the effect of binder viscosity on granule consolidation. The amount of consolidation per collision gives:

$$\frac{\Delta x}{h} \cong 1 - \exp(-St_v) \quad (8.16)$$

where Δx is the reduction in interparticle gap distance h and St_v is the Stokes number ($8\rho u_0 a / 9\mu$), where ρ and a are the density and radius of particle, respectively; u_0 is the collision velocity; and μ is the binder viscosity. Based on Eq. (8.16), increasing the binder viscosity and decreasing the particle size and the collision velocity would decrease the rate of consolidation.

Iveson et al. (1996) proposed a first-order consolidation model assuming that the consolidation rate at any time is inversely proportional to the porosity ε at that time:

$$\frac{d\varepsilon}{dt} = -k(\varepsilon - \varepsilon_{\min}) \quad (8.17)$$

where ε_{\min} is the minimum porosity of the granules and k is the compaction rate constant.

A mechanistic consolidation rate expression used for twin screw granulation by Barrasso et al. (2015b) relating to the particle dynamics using DEM is given:

$$\frac{dV}{dt} = -kV_p C_{\text{impact}} (1 - \exp(-St_v)) \quad (8.18)$$

where V is the particle volume, V_p and C_{impact} are per-particle pore volume and impact frequency, and St_v is the Stokes deformation number.

Layering Kernels

Layering refers to the deposition of fine powders on the surface of a wet granule. The mass balance model considering layering for a batch process follows:

$$\frac{dM_{\text{powder}}}{dt} = F_{\text{powder}}^{\text{in}} - 3G \int_0^{\infty} \frac{M(L)}{L} dL \quad (8.19)$$

and the mass balance model considering layering for continuous process gives:

$$\frac{dM_{\text{powder}}}{dt} = F_{\text{powder}}^{\text{in}} - \frac{M_{\text{powder}}}{t_R} - 3G \int_0^{\infty} \frac{M(L)}{L} dL \quad (8.20)$$

where G is the layering rate, $F_{\text{powder}}^{\text{in}}$ is the flow rate of additional powder stream in both batch and continuous process, t_R is the residence time for the powder, and $M(L)$ and L are the mass of particle and the size of particle, respectively.

Cameron et al. (2005) and Wang et al. (2006) proposed a model to calculate the layering rate according to:

$$G = G_m \frac{M_{\text{powder}}}{kM_{\text{granule}} + M_{\text{powder}}} \exp\left[-a(x_w - x_{wc})^2\right] \quad (8.21)$$

where G_m is the maximum growth rate and M_{powder} and M_{granule} are the mass of fine powder below the lower bound of the particle classes and the mass of granule, respectively. x_w is the moisture content, while x_{wc} is the critical moisture content; k and a are fitting parameters. It is assumed that fine powder is small enough that powder particle size does not play a role in layering. The increase of granule size due to layering is divided among fine powder, liquid, and void components based on their volume fractions. The total increase in the mass of these components into the granule phase is equalized by the decrease in the mass of fine powder and liquid phases. Other forms of layering kernels, which have been applied in the twin screw granulation, could be found elsewhere (Barrasso and Ramachandran 2016).

8.6 Discrete Element Modeling (DEM) of Twin Screw Granulation

The discrete element method (DEM) was first proposed to describe the mechanical behavior of assemblies of spheres for the analysis of rock mechanics (Cundall and Strack 1979). However, DEM simulations are now widespread covering many areas, including but not limited to chemical, mineral, agricultural, and pharmaceutical engineering. DEM is based on an explicit numerical method in which the interaction of particles is monitored contact by contact. The particles are rigid but are subject to local deformation upon contact, and the resulting forces are calculated as a function of the contact law. A fundamental to DEM for the engineering application is the proper selection of the contact force models. Numerous contact models can be used to describe the particle collision behavior such as the hard-sphere model, the Hertz-Mindlin model, and the JKR model. For more details regarding the formulation and contact models, see Zhu et al. (2007). A characteristic feature of this method is that DEM can provide micromechanical insight into the particulate processing which is usually not available from experiments. Due to the rapid advancement of computational power, DEM can serve as an excellent tool to envisage the particle dynamics in the magnitude of millions of particles in the twin screw granulation. This section describes how the particle scale information by means of DEM would be utilized in the population balance model and how the coupling strategy between DEM and PBM could be implemented.

8.6.1 *DEM Simulation of Residence Time Distribution*

Residence time distribution characterization is a key step in the design and scale-up of twin screw granulation (Seem et al. 2015). Among the methods to measure the residence time distribution, DEM has been used to predict velocity spectrum of particles which is then used for the calculation of residence time distribution in the twin screw granulation. Barrasso and Ramachandran (2016) presented the application of DEM in estimating the residence time distribution in compartmental screw elements. It was found out that conveying elements show approximately equal residence times in each compartment. However, the kneading elements exhibited some variation in residence time along the granulator. It is worth noting that kneading elements have longer residence time than the conveying elements, indicating that the kneading elements are prone to inhibit the particle flow.

8.6.2 DEM Simulation of Particle Scale Dynamics

Apart from estimating the residence time distribution, DEM is also coupled with PBM by exploring the particle dynamics (i.e., impact frequency, impact, and collision rates) as input parameters in the rate process kernels. Barrasso and Ramachandran (2016) and Barrasso et al. (2015b) proposed a multiscale mechanistic model incorporating the mechanistic expressions for aggregation, breakage, and consolidation. In particular, these rates were evaluated based on the information from DEM such as particle velocity and collision data. In this study, nucleation and layering were omitted assuming that nuclei have formed with the focus on the later stage. The proposed DEM-PBM model was then used to predict the granulating performance in the twin screw granulator, which were consistent with experimental trends. The effects of screw configuration, material properties, and process parameters on the critical quality attribute were investigated. It was found that the screw configuration is the dominant factor in determining the rate process and product attributes. The mixing elements resulted in more aggregation, breakage, and consolidation as compared to the feed screw. However, qualitative and quantitative validation against the experimental results was lacking in this study. Considering the significant computational cost of running DEM as compared to PBM, this would negatively impact the overall time to solve the DEM-PBM coupling model. Hence, future work is recommended to develop the DEM-based rate kernels in light of particle dynamics with properly calibrated DEM contact models.

8.6.3 DEM-PBM Coupling for Twin Screw Granulation

The main advantage of PBM is the ability to provide a framework that can describe the evolution of a population of particles including subprocess kernels such as coalescence, nucleation, consolidation, and breakage. However, the detailed particle level information for these kernels, for example, spatial variation, is absent in PBM. DEM can provide this missing data of particle collision, particle residence time, and particle flux but is computationally intensive. Considering the complimentary advantages and disadvantages of the respective approaches, significant efforts have been made toward the coupling between DEM and PBM to predict various unit operations such as milling (Carvalho and Tavares 2009; Wang et al. 2012), mixing, and high shear granulation (Lee et al. 2016; Freireich et al. 2011). While there is an increasing trend of applying DEM to simulate the wet granulating process, DEM simulations and its coupling with PBM of twin screw granulator are quite limited in the literature. Barrasso and Ramachandran (2015) implemented bidirectional coupling between PBM and DEM to evaluate collision frequencies and liquid distribution as a proof of concept. Note that liquid droplets were modeled as solid particles with the properties identical to the primary powder

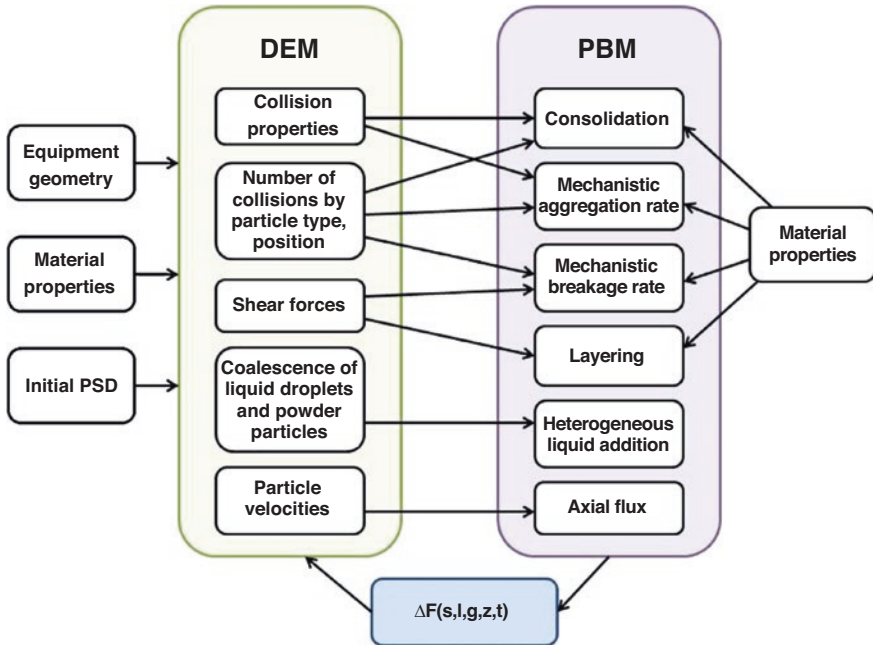


Fig. 8.12 Schematic of multiscale model and information exchange between DEM and PBM (Barrasso and Ramachandran 2015)

particles. A schematic of the coupling approach between DEM and PBM is shown in Fig. 8.12.

As shown in Fig. 8.12, the number of collisions between each pair of bins over the given time interval is recorded from DEM and then transferred to the PBM. The coupling is called two-way coupling on condition that the particle size distribution is updated back to DEM, that is, each time the PBM is solved, the corresponding change in the particle distribution is calculated in the context of DEM. The details of creating particles in DEM could be found in (Barrasso and Ramachandran 2015). The collision between different size ranges was investigated, and it was found that the collision frequency affects the aggregation rate kernel and the evolution of particle size distribution, indicating the need for bidirectional coupling between DEM and PBM. Note that the expression of kernels such as breakage and consolidation is modeled in an empirical way. The mechanistic understanding of these kernels from the perspective of particle level has not been developed in this coupling framework. Along with the advancement of computational capacity in DEM, more efforts are shifted into the development of kernels and PBM-DEM coupling methods. Even though there are many PBM-DEM coupling methods to predict the twin screw granulation (Barrasso and Ramachandran 2016; Barrasso et al. 2015b), the validation and calibration processes of these PBM-DEM models are seldom carried out.

8.7 Concluding Remarks

Twin screw granulation provides a unique approach to continuous wet granulation that gives granules with very different characteristics than those produced by batch high shear wet granulation. It has much shorter residence times, produces more porous granules, and is much less sensitive to formulation properties. The ability to go from development through to full-scale manufacture via scaling out on a time basis reduces risk and gives confidence that granule attributes can be maintained.

The confined nature of the TSG allows it to operate in regime-separated mode. Unlike batch granulation, the granulator geometry is easily changed by adjusting the choice of screw elements and their configuration. This gives almost infinite degrees of freedom, so it is very important to understand the controlling rate processes well in choosing a configuration. It is likely further improvements to screw element geometry and configuration, specifically targeted at granulation, as distinct from extrusion, are possible.

TSG is very amenable to process modeling using a population balance framework either on its own or coupled with particle-scale DEM simulations. As many of the rate processes, such as breakage, are dominated by screw element geometry, models are more robust with fewer arbitrary fitted parameters than those for batch granulation.

References

- Barrasso, D.: Multi-scale modeling of wet granulation process. PhD Thesis, Rutgers University, New Jersey. (2015).
- Barrasso D, Ramachandran R. Multi-scale modeling of granulation processes: bi-directional coupling of PBM with DEM via collision frequencies. *Chem Eng Res Des.* 2015;93:304–17.
- Barrasso D, Ramachandran R. Qualitative assessment of a multi-scale, compartmental PBM-DEM model of a continuous twin-screw wet granulation process. *J Pharm Innov.* 2016;11:231–49.
- Barrasso D, Tamrakar A, Ramachandran R. A reduced order PBM-ANN model of a multi-scale PBM-DEM description of a wet granulation process. *Chem Eng Sci.* 2014;119:319–29.
- Barrasso D, El Hagrasy A, Litster JD, Ramachandran R. Multi-dimensional population balance model development and validation for a twin screw granulation process. *Powder Technol.* 2015a;270:612–21.
- Barrasso D, Eppinger T, Pereira FE, Aglave R, Debus K, Bermingham SK, Ramachandran R. A multi-scale, mechanistic model of a wet granulation process using a novel bi-directional PBM-DEM coupling algorithm. *Chem Eng Sci.* 2015b;123:500–13.
- Cameron IT, Wang FY, Immanuel CD, Stepanek F. Process systems modelling and applications in granulation: a review. *Chem Eng Sci.* 2005;60:3723–50.
- Carvalho RM, Tavares LM. Dynamic modeling of comminution using a general microscale breakage model: Elsevier Inc; Amsterdam. 2009.
- Chablani L, Taylor MK, Mehrotra A, Rameas P, Stagner WC. Inline real-time near-infrared granule moisture measurements of a continuous granulation–drying–milling process. *AAPS PharmSciTech.* 2011;12:1050–5.
- Cundall PA, Strack ODL. A discrete numerical model for granular assemblies. *Géotechnique.* 1979;29:47–65.

- Dhenge RM, Fyles RS, Cartwright JJ, Doughty DG, Hounslow MJ, Salman AD. Twin screw wet granulation: granule properties. *Chem Eng J*. 2010;164:322–9.
- Dhenge RM, Cartwright JJ, Hounslow MJ, Salman AD. Twin screw wet granulation: effects of properties of granulation liquid. *Powder Technol*. 2012a;229:126–36.
- Dhenge RM, Cartwright JJ, Hounslow MJ, Salman AD. Twin screw granulation: steps in granule growth. *Int J Pharm*. 2012b;438:20–32.
- Dhenge RM, Washino K, Cartwright JJ, Hounslow MJ, Salman AD. Twin screw granulation using conveying screws: effects of viscosity of granulation liquids and flow of powders. *Powder Technol*. 2013;238:77–90.
- Djuric D, Kleinebudde P. Impact of screw elements on continuous granulation with a twin-screw extruder. *J Pharm Sci*. 2008;97:4934–42.
- Djuric D, Kleinebudde P. Continuous granulation with a twin-screw extruder: impact of material throughput. *Pharm Dev Technol*. 2010;15:518–25.
- Djuric D, Van Melkebeke B, Kleinebudde P, Remon JP, Vervaet C. Comparison of two twin-screw extruders for continuous granulation. *Eur J Pharm Biopharm*. 2009;71:155–60.
- El Hagrasy AS, Litster JD. Granulation rate processes in the kneading elements of a twin screw granulator. *AICHE J*. 2013;59:4100–15.
- El Hagrasy AS, Hennenkamp JR, Burke MD, Cartwright JJ, Litster JD. Twin screw wet granulation: influence of formulation parameters on granule properties and growth behavior. *Powder Technol*. 2013a;238:108–15.
- El Hagrasy AS, Cruise P, Jones I, Litster JD. In-line size monitoring of a twin screw granulation process using high-speed imaging. *J Pharm Innov*. 2013b;8:90–8.
- Ennis BJ, Tardos G, Pfeffer R. A microlevel-based characterization of granulation phenomena. *Powder Technol*. 1991;65:257–72.
- Fonteyne M, Vercruyse J, Diaz DC, Gildemyn D, Vervaet C, Remon JP, De Beer T. Real-time assessment of critical quality attributes of a continuous granulation process. *Pharm Dev Technol*. 2013;18:85–97.
- Fonteyne M, Arruabarrena J, de Beer J, Hellings M, Van Den Kerkhof T, Burggraeve A, Vervaet C, Remon JP, De Beer T. NIR spectroscopic method for the in-line moisture assessment during drying in a six-segmented fluid bed dryer of a continuous tablet production line: validation of quantifying abilities and uncertainty assessment. *J Pharm Biomed Anal*. 2014;100:21–7.
- Freireich B, Li J, Litster J, Wassgren C. Incorporating particle flow information from discrete element simulations in population balance models of mixer-coaters. *Chem Eng Sci*. 2011;66:3592–604.
- Gao Y, Muzzio FJ, Ierapetritou MG. A review of the Residence Time Distribution (RTD) applications in solid unit operations. *Powder Technol*. 2012;228:416–23.
- Hapgood KP, Litster JD, Smith R. Nucleation regime map for liquid bound granules. *AICHE J*. 2003;49:350–61.
- Hapgood KP, Lveson SM, Litster JD, Liu LX. Granulation. *Handb Powder Technol*. 2007;11:897–977.
- Hill PJ, Ng KM. New discretization procedure for the breakage equation. *AICHE J*. 1995;41:1204–16.
- Hounslow MJ, Ryall RL, Marshall VR. A discretized population balance for nucleation, growth, and aggregation. *AICHE J*. 1988;34:1821–32.
- Hounslow MJ, Pearson JMK, Instone T. Tracer studies of high-shear granulation: II. Population balance modeling. *AICHE J*. 2001;47:1984–99.
- Iveson SM, Litster JD, Ennis BJ. Fundamental studies of granule consolidation Part 1: effects of binder content and binder viscosity. *Powder Technol*. 1996;88:15–20.
- Keleb EI, Vermeire A, Vervaet C, Remon JP. Twin screw granulation as a simple and efficient tool for continuous wet granulation. *Int J Pharm*. 2004;273:183–94.
- Kumar A, Vercruyse J, Toiviainen M, Panouillot PE, Juuti M, Vanhoorne V, Vervaet C, Remon JP, Gernaey KV, De Beer T, Nopens I. Mixing and transport during pharmaceutical twin-screw wet granulation: experimental analysis via chemical imaging. *Eur J Pharm Biopharm*. 2014;87:279–89.

- Kumar A, Alakarjula M, Vanhoorne V, Toiviainen M, De Leersnyder F, Vercruyse J, Juuti M, Ketolainen J, Vervaeet C, Remon JP, Gernaey KV, De Beer T, Nopens I. Linking granulation performance with residence time and granulation liquid distributions in twin-screw granulation: an experimental investigation. *Eur J Pharm Sci.* 2016;90:25–37.
- Lee KT, Ingram A, Rowson NA. Twin screw wet granulation: the study of a continuous twin screw granulator using Positron Emission Particle Tracking (PEPT) technique. *Eur J Pharm Biopharm.* 2012;81:666–73.
- Lee KF, Dosta M, Mcguire AD, Wagner W, Heinrich S, Kraft M, Street P, Street P. Development of a multi-compartment population balance model for high-shear wet granulation with Discrete Element Method New Museums Site. *Comput Chem Eng.* 2016;99:171–84.
- Li H, Thompson MR, O'Donnell KP. Understanding wet granulation in the kneading block of twin screw extruders. *Chem Eng Sci.* 2014;113:11–21.
- Litster JD, Ennis BJ. *The science and engineering of granulation processes*: Kluwer Academic; 2004.
- Liu Y, Thompson MR, O'Donnell KP. Function of upstream and downstream conveying elements in wet granulation processes within a twin screw extruder. *Powder Technol.* 2015;284:551–9.
- Mu B, Thompson MR. Examining the mechanics of granulation with a hot melt binder in a twin-screw extruder. *Chem Eng Sci.* 2012;81:46–56.
- Osorio J, et al. Scaling of continuous twin screw wet granulation. *Am Inst Chem Eng.* 2016;63:921–32.
- Poon JM-H, Immanuel CD, Doyle FJ III, Litster JD. A three-dimensional population balance model of granulation with a mechanistic representation of the nucleation and aggregation phenomena. *Chem Eng Sci.* 2008;63:1315–29.
- Pradhan SU, Sen M, Li J, Litster JD, Wassgren CR. Granule breakage in twin screw granulation: effect of material properties and screw element geometry. *Powder Technol.* 2017;315:290–9.
- Randolph AD, Larson MA. Chapter 3 – the population balance. In: *Theory of particulate processes*; 1971, Elsevier, Amsterdam. p. 41–63.
- Saleh MF, Dhenge RM, Cartwright JJ, Hounslow MJ, Salman AD. Twin screw wet granulation: effect of process and formulation variables on powder caking during production. *Int J Pharm.* 2015;496:571–82.
- Sayin R. *Mechanistic studies of twin screw granulation*. PhD Thesis, Purdue University, Indiana. 2016.
- Sayin R, El Hagrasy AS, Litster JD. Distributive mixing elements: towards improved granule attributes from a twin screw granulation process. *Chem Eng Sci.* 2015a;125:165–75.
- Sayin R, Martinez-Marcos L, Osorio JG, Cruise P, Jones I, Halbert GW, Lamprou DA, Litster JD. Investigation of an 11 mm diameter twin screw granulator: screw element performance and in-line monitoring via image analysis. *Int J Pharm.* 2015b;496:24–32.
- Seem TC, Rowson NA, Ingram A, Huang Z, Yu S, de Matas M, Gabbott I, Reynolds GK. Twin screw granulation – a literature review. *Powder Technol.* 2015;276:89–102.
- Tan MXL, Hapgood KP. Foam granulation: effects of formulation and process conditions on granule size distributions. *Powder Technol.* 2012;218:149–56.
- Thiele W. Twin-screw extrusion and screw design. In *Pharmaceutical Extrusion Technology* (Chapter 4), Edited By Isaac Ghebre-Sellassie, Charles E. Martin, Feng Zhang, James DiNunzio, Taylor and Francis, London. 2003.
- Thompson MR. Twin screw granulation – review of current progress. *Drug Dev Ind Pharm.* 2015;41:1223–31.
- Thompson MR, Sun J. Wet granulation in a twin-screw extruder: implications of screw design. *J Pharm Sci.* 2010;99:2090–103.
- Van Melkebeke B, Vervaeet C, Remon JP. Validation of a continuous granulation process using a twin-screw extruder. *Int J Pharm.* 2008;356:224–30.
- Vercruyse J, Toiviainen M, Fonteyne M, Helkimo N, Ketolainen J, Juuti M, Delaet U, Van Assche I, Remon JP, Vervaeet C, De Beer T. Visualization and understanding of the granulation liquid mixing and distribution during continuous twin screw granulation using NIR chemical imaging. *Eur J Pharm Biopharm.* 2014;86:383–92.

- Wang FY, Ge XY, Balliu N, Cameron IT. Optimal control and operation of drum granulation processes. *Chem Eng Sci.* 2006;61:257–67.
- Wang MH, Yang RY, Yu AB. DEM investigation of energy distribution and particle breakage in tumbling ball mills. *Powder Technol.* 2012;223:83–91.
- Zhu HP, Zhou ZY, Yang RY, Yu AB. Discrete particle simulation of particulate systems: theoretical developments. *Chem Eng Sci.* 2007;62:3378–96.